Journal of Magnetic Resonance 211 (2011) 149–155

Contents lists available at ScienceDirect

Journal of Magnetic Resonance

journal homepage: www.elsevier.com/locate/jmr

Quantitative separation of CEST effect from magnetization transfer and spillover effects by Lorentzian-line-fit analysis of z-spectra

Moritz Zaiß *, Benjamin Schmitt, Peter Bachert

Department of Medical Physics in Radiology, Deutsches Krebsforschungszentrum (DKFZ, German Cancer Research Center), Im Neuenheimer Feld 280, D-69120 Heidelberg, Germany

ARTICLE INFO

Article history:
Received 9 March 2011
Revised 26 April 2011
Available online 15 May 2011

Keywords:
Magnetization transfer
Chemical exchange saturation transfer
Amide proton transfer
Proton transfer rate
Spillover
3-Pool model
Bloch–McConnell equations
z-Spectra modeling

ABSTRACT

Chemical exchange saturation transfer (CEST) processes in aqueous systems are quantified by evaluation of z-spectra, which are obtained by acquisition of the water proton signal after selective RF presaturation at different frequencies. When saturation experiments are performed *in vivo*, three effects are contributing: CEST, direct water saturation (spillover), and magnetization transfer (MT) mediated by protons bound to macromolecules and bulk water molecules. To analyze the combined saturation a new analytical model is introduced which is based on the weak-saturation-pulse (WSP) approximation. The model combines three single WSP approaches to a general model function. Simulations demonstrated the benefits and constraints of the model, in particular the capability of the model to reproduce the ideal proton transfer rate (PTR) and the conventional MT rate for moderate spillover effects (up to 50% direct saturation at CEST-resonant irradiation). The method offers access to PTR from z-spectra data without further knowledge of the system, but requires precise measurements with dense saturation frequency sampling of z-spectra. PTR is related to physical parameters such as concentration, transfer rates and thereby pH or temperature of tissue, using either exogenous contrast agents (PARACEST, DIACEST) or endogenous agents such as amide protons and –OH protons of small metabolites.

1. Introduction

Magnetization transfer (MT) by chemical exchange of protons between small metabolites and bulk water provides a new contrast in MR imaging [1,2]. Chemical exchange saturation transfer (CEST) experiments are commonly used to detect this mechanism through indirect enhancement of the signal of protons in solute metabolites by observing the water resonance, providing information about the microenvironment such as pH and temperature [3].

To observe CEST effects, z-spectra are commonly obtained by acquisition of the water proton signal after selective saturation at different frequencies across the ^{1}H spectral range. The offset frequency $\Delta\omega$ of the saturation pulse is given relative to the water proton resonance (set to $\Delta\omega = 0$). Metabolites useful for CEST must contain so-called labile protons, *i.e.*, protons exchanging at a sufficient rate with other chemical sites in the solution. Important examples are amide protons in the backbone of proteins (APT–CEST [4]) resonant at $\delta = 3.5$ ppm or –OH groups in glycosaminoglycans (gagCEST [5]) with resonances in the range of $\delta = 0.9$–1.9 ppm (water protons at 0 ppm). In saturation experiments with aqueous solutions, at least three effects contribute to the collected z-spectrum: CEST, direct water proton saturation (spillover, DWS), and conventional MT. The challenge is to discriminate CEST effects from the other phenomena.

The common evaluation method is asymmetry analysis of z-spectra around the water peak. This analysis is based on the assumption that direct water saturation and MT effects are symmetric. It requires accurate determination of the resonance frequency of bulk water protons. This can be achieved by field mapping [6], water saturation shift referencing (WASSR) [7], or methods estimating the minimum of high-order-polynomial interpolated z-spectra [4].

For correction and quantification of the measured asymmetry, different post-processing techniques were developed which are based on approximate analytical solutions of the Bloch–McConnell equations for the 2-pool system in equilibrium [6–9]. These solutions yield the proton transfer rate (PTR) after corrections that typically require values for B_0, B_1, as well as knowledge about relaxation and exchange parameters of the involved proton pools.

Because these parameters are hardly accessible *in vivo* this investigation introduces a Lorentzian line shape model for z-spectra which offers access to the ideal CEST proton transfer rate (PTR).

2. Theory

We consider a system ("binary spin bath model") of two proton pools S (solute protons/CEST pool) and W (bulk water protons)

* Corresponding author. Fax: +49 6221 42 3058.
E-mail address: m.zaiss@dkfz.de (M. Zaiß).

1090-7807/$ - see front matter © 2011 Elsevier Inc. All rights reserved.
doi:10.1016/j.jmr.2011.05.001

undergoing chemical exchange (dipolar couplings are neglected) with equilibrium magnetizations M_S^0 and M_W^0, respectively.

The weak-saturation-pulse (WSP) approximation [3] neglects the water-pool RF terms in the two-site Bloch–McConnell equations [10]. Assuming steady state, the reduced water z-magnetization is $\frac{M_{zW}}{M_{zW}^0} = 1 - \mathrm{PTR}$ where the proton transfer rate equals

$$\mathrm{PTR} = \frac{k_{WS}}{R_{1W} + k_{WS}} \cdot \frac{\omega_1^2}{\omega_1^2 + pq + \Delta\omega_S^2 \frac{q}{p}} = \mathrm{PTR}_{\max} \cdot \alpha(\Delta\omega_S) \tag{1}$$

with

$$p = R_{2S} + k_{SW} - \frac{k_{SW}k_{WS}}{R_{2W} + k_{WS}}, \quad q = R_{1S} + k_{SW} - \frac{k_{SW}k_{WS}}{R_{1W} + k_{WS}} \tag{2}$$

given that the system of the two proton pools obeys the rate equation in steady state

$$k_{WS} = \frac{M_S^0}{M_W^0} k_{SW} = f_S \cdot k_{SW} \tag{3}$$

In this set of equations $\Delta\omega_S = \Delta\omega_{RF} - \delta\omega_S$ is the irradiation frequency offset, k_{SW}, k_{WS} are pseudo-first-order rate constants, which determine the chemical exchange for each direction of the exchange process (solute protons → bulk water protons and *vice versa*), f_s is the relative proton fraction, and $R_{1/2,W/S} = 1/T_{1/2,W/S}$ are relaxation rates of the proton pools. In the WSP approximation, direct water saturation (DWS) reduces the z-magnetization of water protons according to:

$$\frac{M_{zW}}{M_{zw}^0}(\Delta\omega) = 1 - \mathrm{DWS} = 1 - \frac{\omega_1^2}{\omega_1^2 + PQ + \Delta\omega_W^2 \frac{Q}{P}} \tag{4}$$

with

$$P = R_{2W} + k_{WS} - \frac{k_{WS}k_{SW}}{R_{2S} + k_{SW}}, \quad Q = R_{1W} + k_{WS} - \frac{k_{WS}k_{SW}}{R_{1S} + k_{SW}}. \tag{5}$$

Inspection of Eqs. (1) and (4) suggests Lorentzian line shapes for PTR and DWS:

$$L(A, \Gamma, \Delta\omega) = \frac{A \cdot \Gamma^2/4}{\Gamma^2/4 + \Delta\omega^2} \tag{6}$$

with maximum A and full width at half maximum (FWHM) Γ. DWS is described by $L_0(A_0, \Gamma_0)$ with

$$A_0 = \frac{\omega_1^2}{\omega_1^2 + PQ} = \mathrm{DWS}_{\max}, \Gamma_0 = 2\sqrt{\omega_1^2 \frac{P}{Q} + P^2} \tag{7}$$

The width Γ_0, which increases with the amplitude B_1 of the RF field, determines the range of influence of direct water saturation.

PTR is described by $L_1(A_1, \Gamma_1)$ with

$$A_1 = \frac{k_{WS}}{R_{1W} + k_{WS}} \cdot \frac{\omega_1^2}{\omega_1^2 + pq} = \mathrm{PTR}_{\max} \cdot \alpha(\Delta\omega_S = 0), \quad \Gamma_1 = 2\sqrt{\omega_1^2 \frac{p}{q} + p^2} \tag{8}$$

Without mutual interference, a simple model for the z-spectrum is

$$\frac{M_{zW}}{M_{zw}^0}(\Delta\omega) = 1 - L_0(\Delta\omega) - L_1(\Delta\omega) \tag{9}$$

In this case, analysis of the asymmetry of the magnetization transfer ratio $\mathrm{MTR}(\Delta\omega) = 1 - \frac{M_{zW}}{M_{zw}^0}(\Delta\omega)$ with respect to the center of L_0 which is a symmetric function would lead to $L_1 = \mathrm{PTR}$. However, the common assumption for the asymmetry of MTR is [11]

$$\mathrm{MTR}_{\mathrm{asym}} = \mathrm{MTR}'_{\mathrm{asym}} + \mathrm{PTR} \cdot \sigma, \tag{10}$$

i.e., it is the sum of the inherent MTR asymmetry $\mathrm{MTR}'_{\mathrm{asym}}$ and the PTR, which is attenuated by the spillover factor σ.

In this paper, the underlying MT is modeled by an additional pool described by a Lorentzian function L_2 yielding MTR′. This function is coupled to the CEST pool function by the multi-pool approximation of Sun [12] to generate the combined transfer rate (CTR):

$$\mathrm{CTR} = \frac{L_1(\Delta\omega) + L_2(\Delta\omega) - 2 \cdot L_1(\Delta\omega)L_2(\Delta\omega)}{1 - L_1(\Delta\omega) \cdot L_2(\Delta\omega)} \tag{11}$$

The spillover factor – which is heuristically calculated with use of the strong saturation pulse approximation [13,14] – is estimated by a probabilistic coupling of the WSP solutions (see Appendix A1). Therefore, CTR and DWS are treated as probabilities for saturation of a spin ensemble:

$$P = \frac{\mathrm{DWS} \cdot (1 - \mathrm{CTR}) + \mathrm{CTR} \cdot (1 - \mathrm{DWS})}{1 - \mathrm{CTR} \cdot \mathrm{DWS}} \tag{12}$$

This yields the new model function

$$f = 1 - P(L_0, L_1, L_2) \tag{13}$$

for Lorentzian-based z-spectra.

3. Materials and methods

All data analysis and simulations were performed in Matlab 7 (The Mathworks, Natick, MA, USA) assuming a static magnetic field $B_0 = 3$ T.

3.1. Numerical solutions

The time course of magnetizations of the spin pools were calculated by means of the numerical Bloch–McConnell matrix solution introduced by Woessner et al. [9]. Simulation parameters were chosen according to results from Stanisz et al. [16], where relaxation times and MT were examined for white matter. Accordingly, for the water pool $T_{1w} = 1084$ ms, $T_{2w} = 69$ ms, $f_W = 1$ were used, for the MT pool $T_{1\mathrm{mt}} = 1000$ ms, $T_{2\mathrm{mt}} = 10$ μs, $k_{\mathrm{mt}W} = 40$ Hz, $f_{\mathrm{mt}} = 0.05$, at an offset of $\delta = -2.43$ ppm.

The approximate modeling of the MT pool by a Lorentzian function instead of the expected super-Lorentzian line shape [17] is possible within a small spectral range (−5 to 5 ppm) around the minimum. We assume that this approximation can be handled for a nearly about four times broader Lorentzian lineshape than the less peaked super-Lorentzian, with respect to T_2. It was taken into account by an altered transversal relaxation time $T'_{2\mathrm{mt}} = 4 \times T_{2\mathrm{mt}} = 40$ μs. For the solute pool, the following parameters were assumed [4]: $T_{1S} = 1000$ ms, $T_{2S} = 160$ ms, $k_{SW} = 50$ Hz, $f_S = 0.2\%$, at an offset $\delta = 1.9$ ppm. Some quantities were varied separately: The offset δ_S of the solute pool was varied from 0.5 to 4 ppm, the amplitude B_1 of the RF field from 0.1 to 4 μT, the transfer rate k_{SW} from 15 to 120 Hz, and the proton fraction f_S from 0.01 to 1%.

Z-spectra were simulated with a sampling increment of 0.05 ppm between −10 and 10 ppm assuming continuous-wave (CW) saturation of $t_{\mathrm{sat}} = 100$-s duration. The simulation of one z-spectrum took ca. 0.03 s, independent of t_{sat}.

3.2. Least-squares fitting

For fitting of simulated z-spectra, the following starting values and boundaries were used (notation: parameter = starting value [lower bound; upper bound]): $A_0 = 1$ [0.95; 1], $\Gamma_0 = 15$ ppm [1; Inf], $\delta\omega_0 = 0$ ppm [−5; 5]; $A_1 = 0.2$ [0; 0.4], $\Gamma_1 = 15$ ppm [1; 5], $\delta\omega_1 = (1.9 \pm 0.1)$ ppm; $A_2 = 0.8$ [0; 1], $\Gamma_2 = 30$ ppm [5; Inf], $\delta\omega_2$

= (−2.43 ± 0.1) ppm. The goodness of fit was observed by SSE (=sum of squared errors). The average fit evaluation time per z-spectrum was ca. 1 s. The fit model functions L_1 and L_2 were compared to the respective theoretical values PTR and MTR′. The variance of the fit evaluation was tested by a Monte-Carlo simulation.

3.3. Monte-Carlo data

To test the stability of the fits against noisy data, a Rician noise distribution according to Ref. [18] was used (see Appendix A2). The relaxation parameters of the simulated systems were the same as noted before. The transfer rate was k_{SW} = 50 Hz, the resonance offset was 1.9 ppm. For each RF amplitude ω_1, noise level σ, and sampling rate *SR*, *n* spectra with random Rician noise were simulated and fitted. Again, A_1 was compared to the directly calculated PTR_{max}. The error bars in the Monte-Carlo plots represent the standard deviation of *n* noisy measurements. The simulation was performed by means of custom-written code of Matlab 7 (The Mathworks, Natick, MA, USA) on an Intel PC with 2.83-GHz CPU. The average evaluation time per z-spectrum of *n* = 50 simulations with noise including fit evaluation was ca. 60 s.

4. Results

Fig. 1a indicates validity of the model function (Eq. (13)) fitted to simulated z-spectra with different RF saturation amplitudes B_1 via SSE of the fits smaller than 10^{-5} even for large values of B_1. The pool functions L_0 and L_2 permit good reproduction of the theoretical opponents DWS and MTR′ with underestimations of the amplitudes of less than 2%. The deviations in FWHM increased with B_1 (Fig. 1b–e). The correlation of L_2 and MTR′ is excellent over the whole examined B_1 range (Fig. 1e and f).

L_1 turned out to be a good estimator (error < 10%) for PTR up to a RF amplitude B_1 = 2 μT (Fig. 1d and f). Therefore, B_1 = 1.5 μT was used in simulations to examine A_1 as a function of f_S, k_{SW}, $\delta\omega_S$, and T_{2W} (Fig. 2). The proposed correction method showed a stable behavior for a large range of solute proton fractions and exchange rates (Fig. 2a and b). Their influence on PTR and L_1 corresponded to expectation from Eqs. (1) and (3). Again, the limit for correction of high spillover – indicated by vanishing asymmetry – was observed when the influence of the water pool was increased: either by moving the solute pool closer than $\delta\omega_S$ = 1 ppm to the water peak (Fig. 2c) or by broadening Γ_0 (approximately $\sim 1/T_{2w}$, Eq. (7)) of water protons with values of T_2 < 30 ms (Fig. 2d). Fig. 2e shows that A_1 also depends

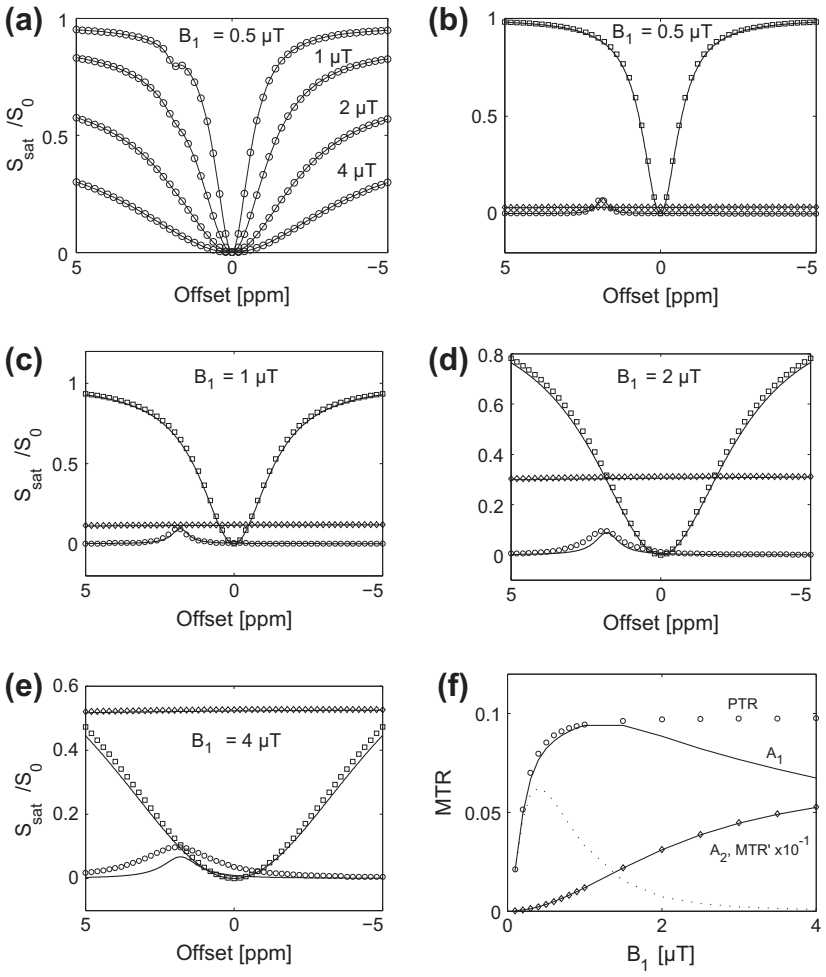

Fig. 1. Simulation of z-spectra and fit results. (a) Lorentzian-based fits (lines) of simulated z-spectra (circles) show good modeling for different RF amplitudes B_1 in the range of 0.5–4 μT; SSE < 10^{-5} in all cases. Figure b–e shows pool functions L_0, L_1, and L_2 (lines) and theoretical results for solute pool (PTR, circles), water pool (1-DWS, squares) and MT pool (MTR′, diamonds), respectively. L_1 and L_2 show good reproduction of the analytical PTR and MTR′ in (b), (c) and (d). Fig. 1e: PTR is underestimated due to high spillover, while MTR′ is reproduced well by L_2. Fig. 1f shows the maximum values of model functions L_1 (=A_1) and L_2 (=A_2) (lines) as a function of B_1 in comparison to PTR (circles) and MTR′ (diamonds). The spillover correction works well up to 1.5 μT where PTR is near its maximum (PTR_{max}). The asymmetry (dotted) shows the expected dilution by spillover and concomitant MT effect and thereby the need for correction.

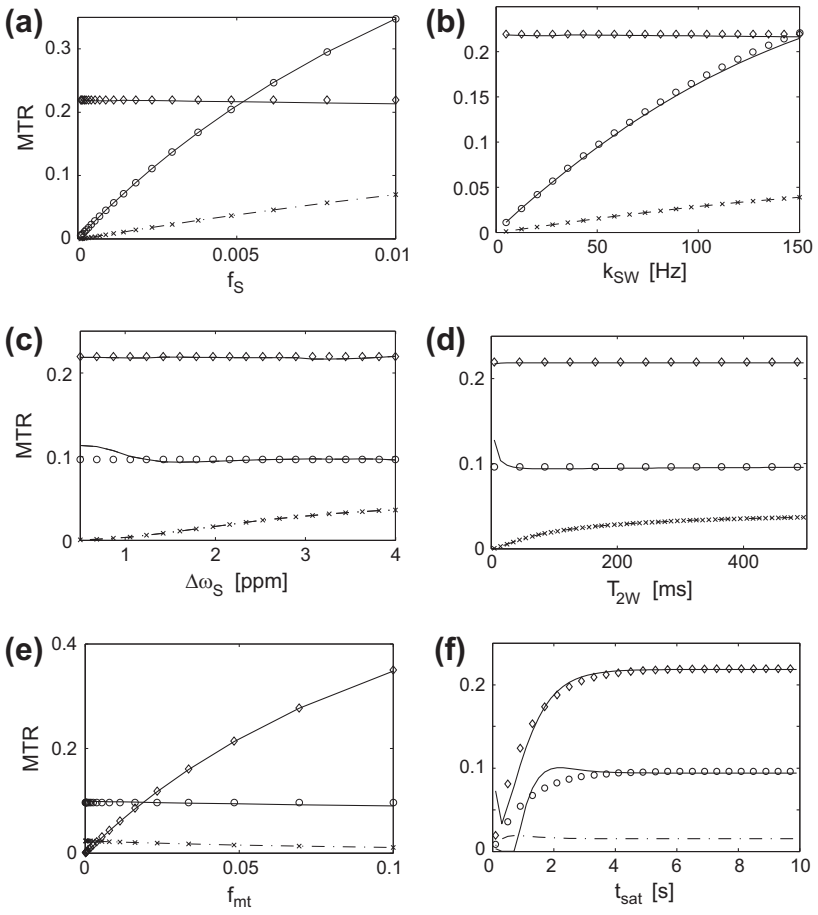

Fig. 2. Results of fit models compared with the theoretical expectation of MTR for solute pool (PTR) and MT pool (MTR′). PTR (circles), MTR′ (diamonds) and pool amplitudes A_1, A_2 (solid lines) simulated with RF amplitude $B_1 = 1.5$ μT as a function of solute proton fraction f_S (a), exchange rate k_{SW} (b), solute proton frequency offset $\delta\omega_S$ (c), transversal relaxation time of water T_{2W} (d) and macromolecular fraction f_{mt} (e). MTR′ prediction by A_2 is excellent for all parameters. PTR prediction works well for a broad range of exchange rates, solute proton fraction, mt proton fractions and $T_{2W} > 50$ ms. PTR prediction fails for too high spillover indicated by the vanishing asymmetry (cross-dotted-dashed) in (c) and (d). (f) If the theoretically justified state of equilibrium is left the fit still yields reliable results for PTR and MTR′ down to $t_{sat} \sim 3 \times T_{1w}$.

on the MT pool concentration: For $f_{mt} = 10\%$ PTR is underestimated by approximately 10%. The same decrease is observed in the asymmetry value. The expected analytic MTR′ was well produced by A_2 for all cases shown in Fig. 2. Although the model is based on the theoretical assumption of equilibrium ($t_{sat} \to \infty$; $dM/dt = 0$), the fit evaluation also works for lower saturation times down to approximately $3 \times T_{1w}$ as shown in Fig. 2f. This is plausible since the temporal variation of PTR and MTR until equilibrium is $\sim$PTR·$(1 - \exp(t_{sat}\cdot(R_{1W} + k_{WS})))$ and $\sim$MTR′·$(1 - \exp(t_{sat}\cdot(R_{1W} + k_{Wmt})))$ and is dominated by T_{1W} [26].

The results of the Monte-Carlo simulation are shown in Fig. 3a, with A_1 plotted as a function of the noise level σ. The standard deviation indicates that $\sigma < 6 \times 10^{-3}$ is necessary for stable and confident fitting. Fig. 3b shows predicted PTR via A_1 as a function of the sampling rate *SR* of z-spectra where rates larger than 3 ppm^{-1} yield reliable results. The evaluations of Fig. 2a, b and e were repeated with additional noise ($\sigma = 5 \times 10^{-3}$), the result is shown in Fig. 3d–f. A_1 seems to be unbiased with a variance of about 5%, A_2 is unbiased with a variance of about 1%. The asymmetry with noise is biased against the asymmetry without noise, though the variance is small (ca. 2%). The variances of A_1 and A_2 for varied T_{2W}, $\Delta\omega_s$ and t_{sat} (Monte-Carlo data not shown) showed similar behavior and were increased in the same range where the simulations in Fig. 2 showed instability. Fit evaluation fails for high spillover ($B_1 > 1.5$ μT) and weak labeling ($B_1 < 0.3$ μT or $k_{sw} <$ 15 Hz), *i.e.*, PTR estimation was vague (Fig. 3c). For high signal-to-noise ratio (SNR), sampling rate, and low spillover, A_1 quantified PTR correctly with an overall standard deviation of about 10%.

5. Discussion

Approximate analytical solutions of the Bloch–McConnell equations, which describe the dynamics of magnetization transfer effects, exist only for the 2-pool case [3,14,15]. For low saturation amplitude B_1, the process of labeling of the CEST pool and the subsequent transfer of labeled protons to the water pool is best described by the WSP approximation [3]. However, for high B_1 amplitudes, the processes of interaction of direct saturation and CEST pool saturation (spillover effect) are best predicted by the "strong-saturation-pulse" (SSP) approximation [15].

A successful prediction of the correct CEST effects for the whole range of B_1 amplitudes is provided by the heuristic combination of WSP and SSP approximations first proposed by Sun et al. [6,13,14]. This approach corrects the asymmetry by different factors for labeling and spillover employing additional information, such as measured values of T_{1W}, T_{2W}, $B_{1\ and\ \Delta B0}$. Additionally, T_{1S}, T_{2S}, k_{SW}, and f_S, which are difficult to obtain, are used implicitly to reconstruct the ideal PTR on resonance.

In the present paper, Lorentzian pool functions based on the WSP solution are likewise merged heuristically to obtain a model for z-spectra that yields PTR values by a functional combination

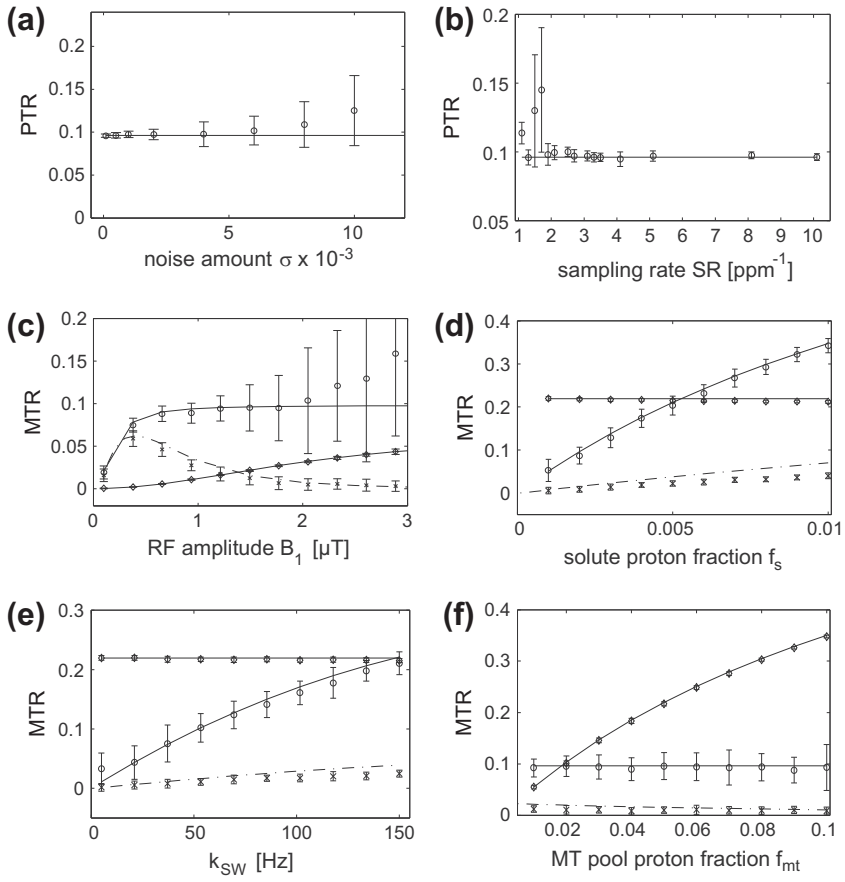

Fig. 3. Results of Monte-Carlo simulation. PTR, MTR′(solid lines), A_1 (circles), and A_2 (diamonds) obtained by fit of $n = 50$ simulated z-spectra per system parameter, each altered by Rician noise. Ideal and fit results as a function of (a) noise level σ, (b) sampling rate SR, (c) RF amplitude B_1, (d) solute proton fraction f_s, (e) exchange rate k_{SW}, and (f) MT proton fraction f_{mt}. PTR prediction fails for $\sigma > 5 \times 10^{-3}$, SR < 3/ppm, and too small CEST effect due to slow exchange (k_{SW} < 15 Hz), spillover or inefficient labeling (0.3 μT < B_1 < 1.5 μT). This agrees with results shown in Fig. 1f. Figures d–f demonstrate the unbiased and accurate (within 10%) estimation of PTR and MTR′ for the varied parameters f_s, k_{SW} and f_{mt} also for noisy data (cf. Fig. 2).

of unperturbed solutions, and reproduces the first-order spillover effects. The transition from T_1, T_2, k, and ω_1 to a new set of parameters, i.e. A and Γ, simplified the modeling of z-spectra and therefore led directly to the fundamental parameters PTR and MTR′.

In contrast to the method proposed by Sun et al. [6], no further parameters other than A and Γ must be known because all information is extracted from the z-spectrum. Furthermore, the concomitant conventional MT effect could be modeled through adding of another pool, which was incorporated into the model function using the multi-pool approach of Sun [12]. The resulting heuristic 3-pool model enabled analytical least-squares fitting of the data, which is much faster than numerical fits. Since transfer terms between CEST and MT pool are neglected, it is not a full 3-pool model, but rather a dual 2-pool model for the entire z-spectrum. As shown by Fig. 1, the spillover correction is ineffective for high B_1 amplitudes. In this case, attenuation of the CEST effect by the direct water saturation is stronger than modeled by our probabilistic approach. One possible explanation may be the invalidity of the implicit assumption of independence of direct and indirect saturation in the case of full saturation. Labeling of the CEST pool can be influenced by transferred saturation from the water pool. Advanced models may take this into account including quadratic and higher-order terms of L_0 and CTR in the model function.

Nevertheless, below the spillover threshold (approx. 50% direct saturation at CEST resonance), the model evaluation is able to reconstruct both PTR and MTR′ with good precision.

However, due to the use of nonlinear least-squares fitting, in addition to noisy data, stability of prediction had to be proven. The reliable determination of nine independent parameters requires high SNR and sampling rate, which might compromise the *in vivo* application due to long scan times; these are the same shortcomings which also arise for common Bloch–McConnell evaluation. This can be resolved by measuring T_1 and T_2, which determine P and Q and hence Γ. Moreover, the absolute and relative position of the Lorentzian pool functions could be obtained by means of an additional B_0 scan. Alternatively, the proposed model could be used as a correction tool for common asymmetry analysis by calculating the asymmetry of Eq. (12) using additional information for the pools L_0 and L_2. However, the information of the almost symmetric MT pool would then be lost.

Additional measurements at different B_1 amplitudes would allow to extrapolate PTR(B_1) to the fully labeled PTR_{max}. This may also permit determination of p and q which then provides a B_1 correction by using Eq. (1) similar to the approach of Sun et al. [6].

The present evaluation method strengthens the significance of the dependence of CEST contrast on the exchange rate and mobile proton concentration due to elimination of interference with spillover and MT effect. However, our method is not able to separate directly the influence of k and f on PTR or the cause of changes in k (resulting from changes of temperature or pH). Nevertheless, for APT it could be shown that at constant temperature PTR clearly reflects changes of pH in the physiological range [13]. Li et al. showed that at constant pH PARACEST PTR correlates with temperature [25]. Sun et al. proposed a method for measuring k independently of f by means of the optimal B_1 amplitude for spillover-diluted CEST [24]; another method applicable to fast exchanging PARACEST

agents was suggested by Dixon [23] using a series of varying B_1 values. The latter method, which assumes that there is no spillover or MT effect, could benefit from our correction for the application in the general case.

B_0 errors, which are the fundamental problem of asymmetry analysis of z-spectra, are avoided by a fit evaluation with flexible water pool frequency. Of course, B_0 inhomogeneities should be small enough ($\Delta B_0 \sim$ <1 ppm) that water or CEST pool are not undersampled or outside the measured range. Fitting with a model function, which also takes into account values measured at large offsets from the minimum, is more appropriate than interpolation of z-spectra by spline [19] or polynomial functions [4].

In the present model function contributions from lipid protons were not included. Therefore, data with lipid saturation effects (at around −2.34 ppm) would lead to misinterpreted L_0 and/or L_2. However, L_1 (=PTR) should be changed only slightly by the spillover and MT correction. In contrast to asymmetry analysis no cancelation of lipid effects by CEST effects with positive chemical shift occurs. Furthermore, the lipid pool could be modeled by an additional pool function L_3 with appropriate line shape, which could be added (in an adequate manner) to a four-pool fit model function to describe z-spectra with lipid contributions correctly.

For analysis of pulsed saturation experiments in clinical MRI scanners where the spin systems do not reach equilibrium [20,21] the present Lorentzian-based model is not valid. First of all, the line shape of the pool functions is changed due to the line shape of the saturation pulse; second, Zu et al. [22] demonstrated that for pulsed CEST experiments with different pulse widths the same RF saturation power and the same amount of direct water saturation can lead to different intensity of the CEST effect. This shows that there cannot be a general model for spillover correction of pulsed CEST data for all pulse widths. Nevertheless, for one selected pulse width the probabilistic approach of combining the respective pool functions, which allowed to describe the weakening of cw CEST effects, may yield an approximation of the interaction effects and thus give a tool for correction of PTR. However, pool functions for partially saturated proton pools have to be found for the correct description of this case.

The proposed evaluation would also be interesting for PARACEST, where spillover effects are moderate due to large chemical shifts, but conventional MT still has to be considered [3,17]. Here, L_2 must be modeled by a super-Lorentzian lineshape.

6. Conclusion

In this study, the weak saturation pulse approximation was used to combine effects of direct saturation, solute proton pool saturation, and conventional MT analytically to derive an appropriate model function for z-spectra obtained in *in vivo* CEST experiments. This modeling was shown to be able to reconstruct ideal PTR and MTR′ from fitted z-spectra for moderate spillover effects, and z-spectra acquired with high SNR and dense offset sampling.

Acknowledgement

We like to thank Shanrong Zhang for kindly sharing his CESTfit program with us.

Appendix A

A1. Probabilistic combination of direct water saturation and magnetization transfer ratio

With DWS, the probability for a spin packet to be saturated directly, and MTR, the probability for a spin packet to be saturated and then transferred to the water pool, the total probability for saturation of a spin packet is

$$P = \mathrm{DWS}\cdot(1-\mathrm{MTR}) + \mathrm{MTR}\cdot(1-\mathrm{DWS}) \tag{A.1}$$

The probability for no saturation is

$$Q = (1-\mathrm{MTR})\cdot(1-\mathrm{DWS}) \tag{A.2}$$

hence

$$\frac{P}{Q} = \frac{\mathrm{DWS}\cdot(1-\mathrm{MTR}) + \mathrm{MTR}\cdot(1-\mathrm{DWS})}{(1-\mathrm{MTR})\cdot(1-\mathrm{DWS})} \tag{A.3}$$

Assuming $Q = 1 - P$ one obtains

$$P = \frac{\mathrm{DWS}\cdot(1-\mathrm{MTR}) + \mathrm{MTR}\cdot(1-\mathrm{DWS})}{1-\mathrm{MTR}\cdot\mathrm{DWS}} \tag{A.4}$$

A2. Simulation of Rician distribution

The noise of MRI signals is given by a Rician distribution [18]

$$p(M) = \frac{M}{\sigma^2}\exp\left(-\frac{(M^2+A^2)}{2\sigma^2}\right)\cdot I_0\left(\frac{MA}{\sigma^2}\right) \tag{A.5}$$

where A is the pixel intensity in the absence of noise and M is the measured data. I_0 is the modified zero-order Bessel function of the first kind and σ denotes the standard deviation of the Gaussian noise in the real and the imaginary images (which we assume to be equal). This noise can be simulated by Gaussian-distributed random values because $R \propto Rice(A,\sigma)$ if $R = \sqrt{X^2+Y^2}$, where X and Y are normally distributed with $X \propto N(A*\cos(\theta),\sigma), Y \propto N(A*\sin(\theta),\sigma)$. Without loss of generality we assume $\theta \equiv 0$. The measured data M was simulated by z-spectra data A and a normally distributed random function rdm(mean, std) as $M = \sqrt{(A+\mathrm{rdm}(0,\sigma)^2 + \mathrm{rdm}(0,\sigma)^2}$.

References

[1] S. Forsén, R.A. Hoffman, Study of moderately rapid chemical exchange reactions by means of nuclear magnetic double resonance, Journal of Chemical Physics 39 (11) (1963) 2892.
[2] S.D. Wolff, R.S. Balaban, NMR imaging of labile proton exchange, Journal of Magnetic Resonance 86 (1) (1990) 164–169 (1969).
[3] J. Zhou, P.C.V. Zijl, Chemical exchange saturation transfer imaging and spectroscopy, Progress in Nuclear Magnetic Resonance Spectroscopy 48 (2–3) (2006) 109–136.
[4] J. Zhou, J. Payen, D.A. Wilson, R.J. Traystman, P.C.M.V. Zijl, Using the amide proton signals of intracellular proteins and peptides to detect pH effects in MRI, Nature Medicine 9 (8) (2003) 1085–1090.
[5] W. Ling, R.R. Regatte, G. Navon, A. Jerschow, Assessment of glycosaminoglycan concentration in vivo by chemical exchange-dependent saturation transfer (gagCEST), Proceedings of the National Academy of Sciences of the United States of America 105 (7) (2008) 2266–2270.
[6] P.Z. Sun, C.T. Farrar, A.G. Sorensen, Correction for artifacts induced by B_0 and B_1 field inhomogeneities in pH-sensitive chemical exchange saturation transfer (CEST) imaging, Magnetic Resonance in Medicine: Official Journal of the Society of Magnetic Resonance in Medicine/Society of Magnetic Resonance in Medicine 58 (6) (2007) 1207–1215.
[7] M. Kim, J. Gillen, B.A. Landman, J. Zhou, P.C.M.V. Zijl, Water saturation shift referencing (WASSR) for chemical exchange saturation transfer (CEST) experiments, Magnetic Resonance in Medicine: Official Journal of the Society of Magnetic Resonance in Medicine/Society of Magnetic Resonance in Medicine 61 (6) (2009) 1441–1450.
[8] J. Zhou, D.A. Wilson, P.Z. Sun, J.A. Klaus, P.C.M.V. Zijl, Quantitative description of proton exchange processes between water and endogenous and exogenous agents for WEX, CEST, and APT experiments, Magnetic Resonance in Medicine: Official Journal of the Society of Magnetic Resonance in Medicine/Society of Magnetic Resonance in Medicine 51 (5) (2004) 945–952.
[9] D.E. Woessner, S. Zhang, M.E. Merritt, A.D. Sherry, Numerical solution of the Bloch equations provides insights into the optimum design of PARACEST agents for MRI, Magnetic Resonance in Medicine: Official Journal of the Society of Magnetic Resonance in Medicine/Society of Magnetic Resonance in Medicine 53 (4) (2005) 790–799.
[10] H.M. McConnell, Reaction rates by nuclear magnetic resonance, Journal of Chemical Physics 28 (3) (1958) 430.
[11] J. Hua, C.K. Jones, J. Blakeley, S.A. Smith, P.C.V. Zijl, J. Zhou, Quantitative description of the asymmetry in magnetization transfer effects around the

water resonance in the human brain, Magnetic Resonance in Medicine 58 (4) (2007) 786–793.
[12] P.Z. Sun, Simplified and scalable numerical solution for describing multi-pool chemical exchange saturation transfer (CEST) MRI contrast, Journal of Magnetic Resonance 205 (2) (2010) 235–241.
[13] P.Z. Sun, A.G. Sorensen, Imaging pH using the chemical exchange saturation transfer (CEST) MRI: correction of concomitant RF irradiation effects to quantify CEST MRI for chemical exchange rate and pH, Magnetic Resonance in Medicine: Official Journal of the Society of Magnetic Resonance in Medicine/Society of Magnetic Resonance in Medicine 60 (2) (2008) 390–397.
[14] P.Z. Sun, P.C. van Zijl, J. Zhou, Optimization of the irradiation power in chemical exchange dependent saturation transfer experiments, Journal of Magnetic Resonance 175 (2) (2005) 193–200.
[15] E. Baguet, C. Roby, Off-resonance irradiation effect in steady-state NMR saturation transfer, Journal of Magnetic Resonance 128 (2) (1997) 149–160.
[16] G.J. Stanisz, E.E. Odrobina, J. Pun, M. Escaravage, S.J. Graham, M.J. Bronskill, R.M. Henkelman, T_1, T_2 relaxation and magnetization transfer in tissue at 3 T, Magnetic Resonance in Medicine 54 (3) (2005) 507–512.
[17] A.X. Li, R.H.E. Hudson, J.W. Barrett, C.K. Jones, S.H. Pasternak, R. Bartha, Four-pool modeling of proton exchange processes in biological systems in the presence of MRI-paramagnetic chemical exchange saturation transfer (PARACEST) agents, Magnetic Resonance in Medicine: Official Journal of the Society of Magnetic Resonance in Medicine/Society of Magnetic Resonance in Medicine 60 (5) (2008) 1197–1206.
[18] H. Gudbjartsson, S. Patz, The Rician distribution of noisy MRI data, Magnetic Resonance in Medicine: Official Journal of the Society of Magnetic Resonance in Medicine/Society of Magnetic Resonance in Medicine 34 (6) (1995) 910–914.
[19] J. Stancanello, E. Terreno, D.D. Castelli, C. Cabella, F. Uggeri, S. Aime, Development and validation of a smoothing-splines-based correction method for improving the analysis of CEST-MR images, Contrast Media Mol. Imaging 3 (4) (2008) 136–149.
[20] H. Zhu, C.K. Jones, P.C.M. van Zijl, P.B. Barker, J. Zhou, Fast 3D chemical exchange saturation transfer (CEST) imaging of the human brain, Magnetic Resonance in Medicine n/a–n/a (2010). doi:10.1002/mrm.22546.
[21] B. Schmitt, M. Zaiß, J. Zhou, P. Bachert, Optimization of pulse train presaturation for CEST imaging in clinical scanners. Magnetic Resonance in Medicine, in press. doi:10.1002/mrm.22750.
[22] Z. Zu, K. Li, V.A. Janve, M.D. Does, D.F. Gochberg, Optimizing pulsed-chemical exchange saturation transfer imaging sequences. Magnetic Resonance in Medicine (2011). doi:10.1002/mrm.22884.
[23] W.T. Dixon, A concentration-independent method to measure exchange rates in PARACEST agents, Magnetic Resonance in Medicine 63 (2010) 625–632.
[24] P.Z. Sun, Simultaneous determination of labile proton concentration and exchange rate utilizing optimal RF power: radio frequency power (RFP) dependence of chemical exchange saturation transfer (CEST) MRI, JMR 202 (2010) 155–161.
[25] A.X. Li, A sensitive PARACEST contrast agent for temperature MRI: Eu^{3+}-DOTAM-glycine (Gly)-phenylalanine (Phe), Magnetic Resonance in Medicine 59 (2008) 374–381.
[26] M.T. McMahon, Quantifying exchange rates in chemical exchange saturation transfer agents using the saturation time and saturation power dependencies of the magnetization transfer effect on the magnetic resonance imaging signal (QUEST and QUESP): Ph calibration for poly-L-lysine and a starburst dendrimer, Magnetic Resonance in Medicine 55 (2006) 836–847.